

# Effect of FSW Parameters on Hook formation, Microstructure and Fracture Strength of Al, Mg alloys

<sup>1</sup>Shubhavardhan R N, <sup>2</sup>M.M Rahman

Department of Mechanical Engineering

<sup>1</sup>University of Saskatchewan, Saskatoon, Canada, <sup>2</sup>DUET, Gazipur, Bangladesh.

**Abstract**— Friction stir welding (FSW) is a solid-state joining technique which can be used for joining not only traditionally weldable aluminum alloys but also high strength aluminum and other metallic alloys that are hard to weld using conventional fusion welding processes. During (friction stir lap welding) FSLW of similar metallic alloys, a part of the original lapping interface between the plates is lifted up due to a specific material flow induced by the rotating threaded tool pin, taking a hook shape. Such a hook in a FSL welds often provides a favorable site for crack propagation under loading and thus adversely affects  $\sigma_{Lap}$ . Furthermore, FS heat causes local softening but grain refinement by dynamic recrystallization contributes to hardening in stir zone. Thus strength is location dependent. The nature (shape and continuity) of hooks in FSL welds of similar alloys have not been discussed well in literature. Thus, the aim of the present research is to provide thermomechanical explanation on how  $\omega$  and  $v$  affects hook formation during FSLW; to understand how hooking, FS softening, stress concentration and local deformation mechanisms (under loading) relate to fracture strength of Al and Mg FSL welds.

**Index Terms**—Aluminum alloy, Magnesium alloy, Friction stir lap welding, Fracture strength, FSW parameters

## I. INTRODUCTION

Friction stir welding (FSW) is a solid state joining process and melting/solidification related defects of fusion welding are avoided. Thus, since it was invented in early 1990s [1], FSW has been applied quite widely [2]. Many aspects of FSW have been studied extensively and comprehensively reviewed [3-9]. The majority of FSW studies have been based on butt joint geometry. Lap joint configuration is also widely used in conventional welding and friction stir lap welding (FSLW) should potentially be applied widely, particularly in automotive and aerospace industries. Fig. 1a illustrates FSLW during which a section of lapping surfaces of the top and bottom plates is stirred and mixed in the stir zone (SZ) thus forming a weld behind the tool. During FSLW of Al-to-Al, Mg-to-Mg or steel-to-steel, material flow affects the un-welded original lapping interface (referred to as un-welded lap hereafter) on both the retreating side and the advancing side. As illustrated in Fig. 1b, upward flow on advancing site of SZ behind the tool drives the material upward and thus a portion of the un-welded lap curves (hooks) up, forming a hook. The hook can be viewed as crack that may orientate favorably for crack growth under loading in service. In the studies of hooking and its effect on joint properties, a hook size ( $h$ ) refers to the vertical distance of the hook [10-16] and there has been little attention paid to the actual shape and the quality (continuity) of the hook.

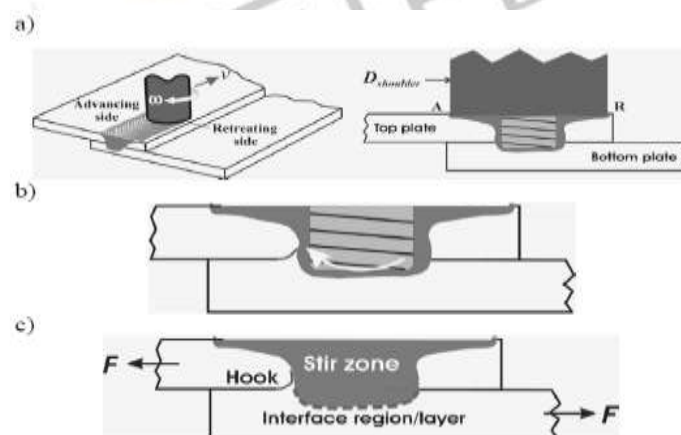


Fig.1. Schematics illustrations of (a) FSLW and (b) material flow up-lifting un-welded lap thus hooking during FSLW and (c) forces applied to a welded joint during subsequent mechanical testing.

The use of a higher tool rotational speed ( $\omega$ ) or a lower welding speed ( $v$ ) has been shown to result in a larger  $h$  [14-16], although the detailed thermo mechanical reasons have not been more accurately explained. It is generally understood [10-16] that a high  $h$  value can result in a lower strength of the lap weld. However, without sufficiently detailed quantification of hooking, a better estimation on how hooking affect weld strength cannot be made. A better understanding on hooking and how it affects weld strength should be critically important for FSLW to be used in automobile and aerospace manufacturing industries.

## II. EXPERIMENTAL PROCEDURE

Work piece materials were A6060-T5 aluminum alloy plates 3 mm for Al-to-Al, 2.5 mm AZ31B-H24 magnesium alloy. Both top and bottom plates were 200 mm long and 100 mm wide. Tools were made using H13 tool steel and the left-hand threads of the pins were made with a 1 mm pitch and a 0.6 mm actual depth. The diameter of the concave shoulder was 18 mm for Al-to-Al and Mg-to-Mg FSLW. A tool tilt angle ( $\Theta$ ) of 2.5 was used. In the present experiments,  $v$  ranged from 20 to 630 mm/min and  $\omega$  ranged from 500 to 2000 rpm. For the work reported here, the penetration depth ( $D_p$  in Fig. 2) was  $\sim 1$  mm for FSLW of Al-to-Al and Mg-to-Mg. Tensile shear testing of welded specimens were performed and the effect of loading geometry on local deformation was investigated using SEM/EBSD and by detailed fractographic observation. Finite element method (FEM) modeling was conducted to investigate the stress distribution and stress relaxation due to local deformation during tensile shear testing. Thus, how stress concentration/relaxation together with FS softening and hooking contributes to the final  $\sigma_{Lap}$  could be studied in detail.

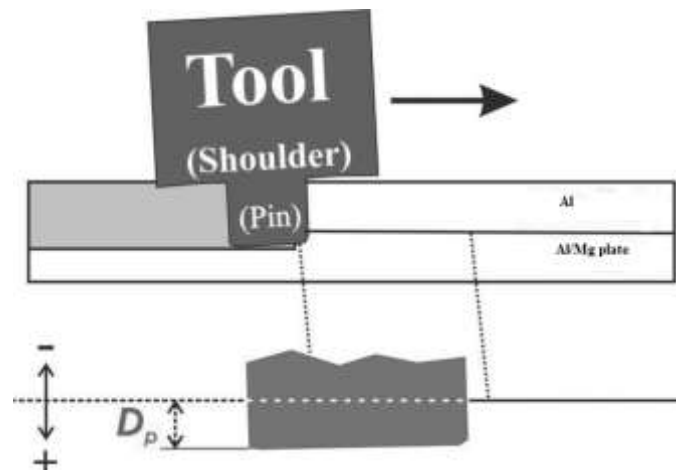


Fig.2. Schematic illustration of tool positioning during FSLW showing pin penetration depth

## III. RESULTS AND DISCUSSIONS

### *Al- Al FSLW microstructure and fracture strength:*

Fig. 3 illustrates the general features of hooking and in the figure SZ has been outlined and the hook outside, but very close to, SZ is shown. Material flow in the lower part of SZ during FS with the direction as indicated in the figure pushed up a small portion of the un-welded lap, thus forming the hook. These features are in common with those already described in literature [13-15]. It should be noted that the bell shape of the SZ is primarily the consequence of the combination of the pin related bottom-mid flow and the shoulder related mid-upper flow.

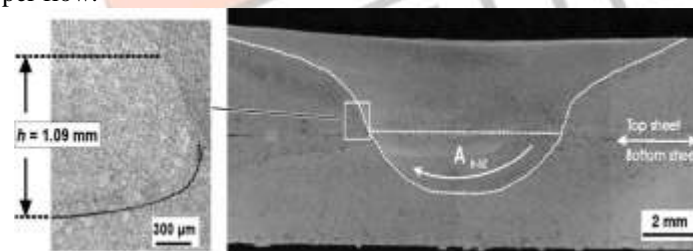


Fig.3. Cross sectional view of an A6060 weld made using  $\omega = 1,000$  rpm and  $v = 224$  mm/min displaying a hook and indicating FS flow direction

In Fig.4, microstructures of the hook are further shown. The shape (elongated) and orientation (more dominantly red with orientation shown by the inverse pole figure) of grains in the area including the edge of SZ and thermomechanical affected zone (TMAZ) are clearly different from those in heat affected zone (HAZ) which are largely equiaxed with a different texture (green/blue). It can thus be suggested that not only there is an upward flow induced by the pin during FS, there is a sideward flow (deformation) in the mid-upper region caused by the tool shoulder and the grains were deformed and elongated.

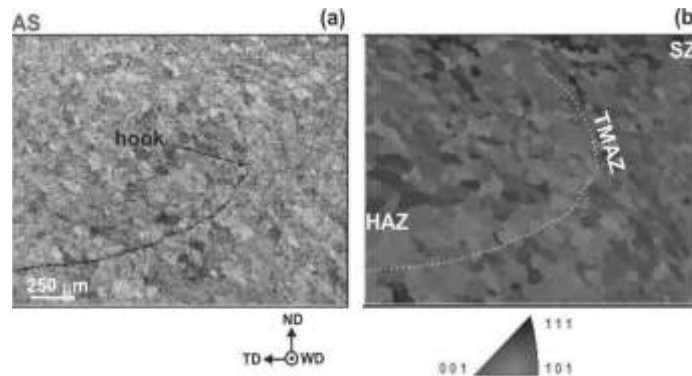


Fig.4. Hook region in an A6060 weld made using  $\omega = 1,000$  rpm and  $v = 224$  mm/min shown by (a) optical micrograph and (b) EBSD orientation map

The upward flow that first causes a hook to form and then the sideward flow shapes the hook to its final orientation, respectively, can thus be suggested and summarized in Fig. 5. The pin related bottom flow first lifts the un-welded lap primarily in TMAZ upward which is the flow direction in TMAZ. Later, in the mid-upper region of SZ/TMAZ, the rotating shoulder forges the material not only flowing forward but also sideward due to the material in the upper region being sheared from the retreating side to the advancing side. The upper portion of a hook is thus also forged and sheared sideward and away (from the pin). The size and orientation of a hook thus depend on the intensities of these two flows.

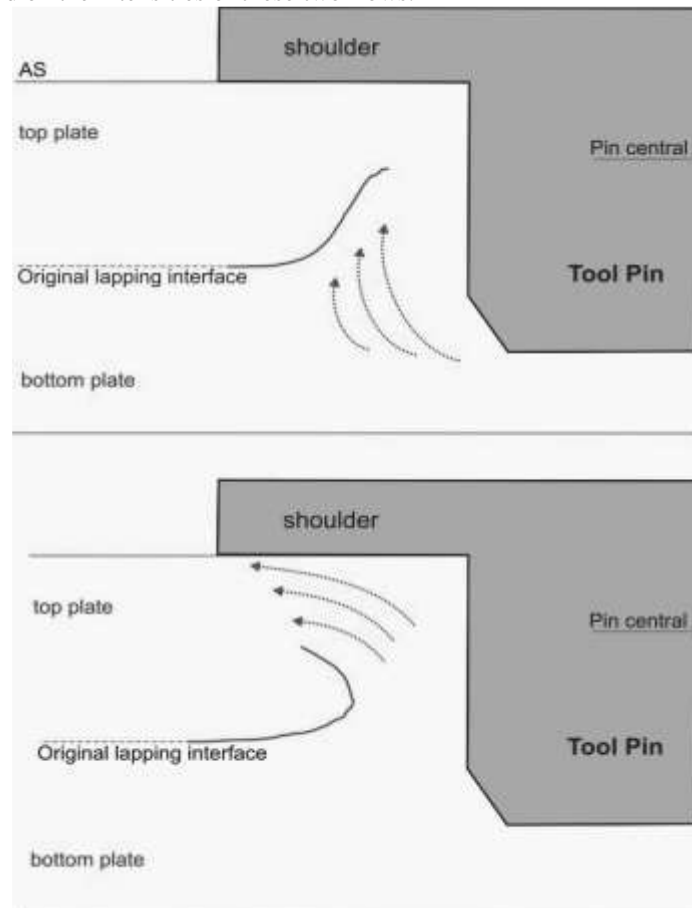


Fig.5. Schematic illustration of pin and shoulder related upward flow (top) and sideward flow (bottom), respectively

When  $\omega$  increased from 500 rpm to 1,000 rpm, the increase in  $Asz$  clearly increased  $h$ , while the sideward flow was strong for both case, resulting in the hooks curving and pointing away. The further increase from 1,000 rpm to 2,000 rpm increased further  $Asz$ , but  $h$  has remained the same. It should be noted that if any of the hooks was folded back to the original lapping interface location, the end of the hook would not reach the tool pin. This means a part of the original lapping interface has disappeared. The reason for missing a portion of the original lapping interface becomes clear when features of hooks are examined more closely. Images of two hooks are given in Fig. 6. The two measured  $h$  values are almost equal, but the two hooks are very different in both the shape and “quality”. On shape, hook A curves significantly more away from the vertical direction than hook B, as expressed by the  $\gamma$  values to be  $70^\circ$  and  $46^\circ$ , respectively. This would mean a stronger sideward flow (more deformation sideward) for hook A. A large amount of deformation (strain) has resulted in the lapping interface becoming more discontinuous and locally closed. Discontinuity is more frequent towards the end. Thus it can be expected that a strong sideward flow should

result in part of the section towards the end having closed completely. This is the reason why part of the original lapping interface has disappeared.

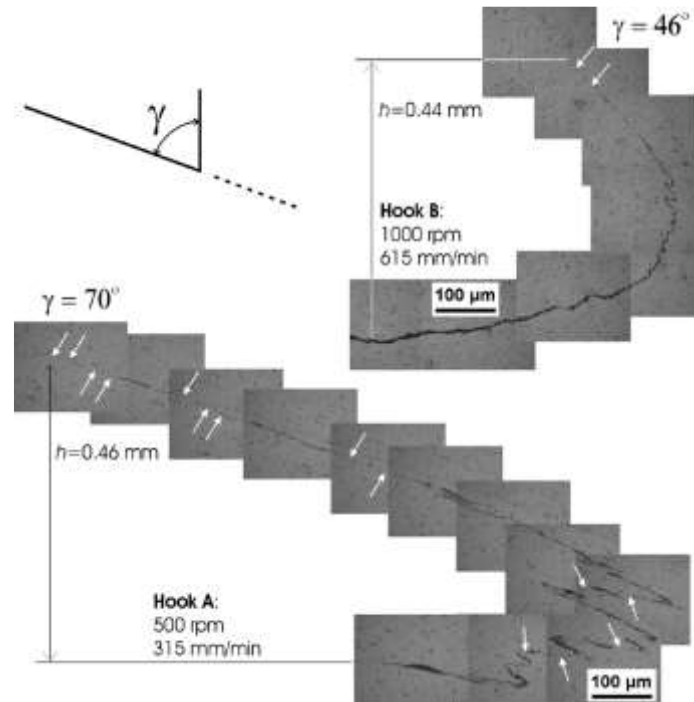


Fig.6. Micrographs of two hooks of A6060 welds with different hook angles ( $\gamma$ ) and local hook discontinuities as pointed to by arrows

Strength ( $F_m/w_s$ ) values plotted as a function of  $h$  are given in Fig.7 . As a comparison, the range of  $F_m/w_s$  values of FS bead-on-plate samples using the same alloy plate is provided. A higher  $\omega$  value or a lower  $v$  value normally results in lower  $F_m/w_s$  for these bead-on-plate samples. For these samples fracture locations were all in HAZ, which was also the fracture location for low  $h$  samples of FSL welds. For samples with high  $h$  values, samples failed by crack propagation from the hook. Data in Fig.7 have suggested that there is a transition point ( $ht$ ) at  $\sim 0.9$  mm. Below  $ht$ ,  $F_m/w_s$  decreases only slightly as  $h$  increases and above  $ht$ ,  $F_m/w_s$  decreases sharply as  $h$  further increases.

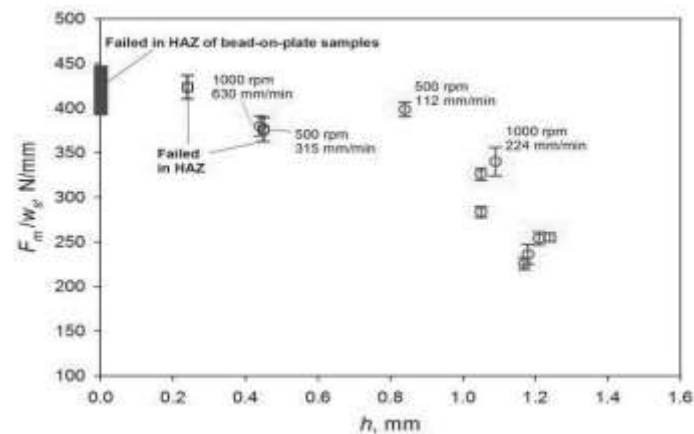


Fig.7. Strength values plotted as a function of hook size for A6060 welds. Some samples failed in HAZ as indicated and marked blue and other samples (red) cracked from hook

We now return to the observation that  $F_m/w_s$  is not affected by the large stress concentration present in the region around the end of the hook. Stress concentration for tensile-shear testing using a lap joint geometry with  $h = 0$  is illustrated in Fig. 8. The applied load is 50 MPa and the highest stress value has reached 170 MPa, which is sufficiently high for annealed A6060 to plastically deform. Then the local deformation should result in local bending thus straightening the top and bottom pieces to align more in the loading direction. This new alignment should then reduce considerably or eliminate the stress concentration.

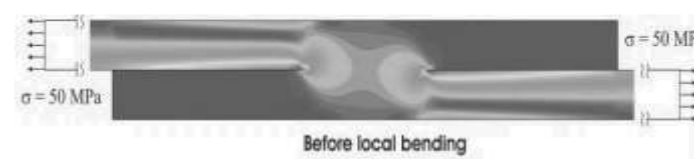


Fig.8. Simulation results showing distribution of effective stress in the lap location during tensile-shear testing. Red  $\sim 170$  MPa and dark blue 0 MPa

Two tested samples shown in Fig.9 illustrate the local bending and sample strengthening. When stress concentration is reduced to a very low level, deformation and fracture of the sample will then be away from the region of the hook if thinning effect is not strong. In the case of deformation and fracturing in HAZ of a lap sample, such as the top sample in Fig.9, the strength should not be significantly different from that of a bead-on-plate sample. Thus there is no reason for a significant reduction in weld strength. This is why strength value of the weld with  $h = 0.24$  mm is well within the range of strength values of bead-on-plate samples.

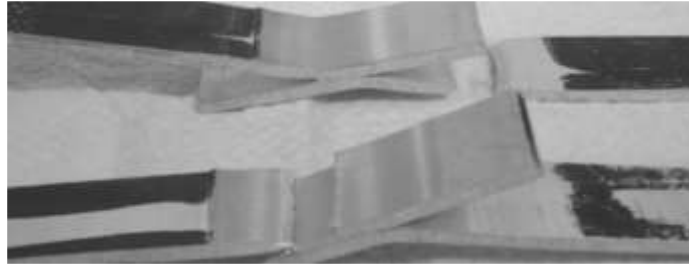


Fig.9. Tensile-shear tested samples of A6060 welds showing fracture in HAZ (top) and in hook region (bottom), after strengthening

#### **Mg-Mg alloy microstructure and fracture strength:**

A high  $h$  hook of an AZ31B weld is shown in Fig. 10. The pin induced upward flow very effectively lifted the un-welded lap a long distance up. But, the sideward flow caused by the shoulder is very different to that during Al alloy FSLW and is very weak during this Mg alloy FSLW. This weak sideward flow has resulted in  $\gamma \ll 0$ .



Fig.10. Cross sectional view of an AZ31B weld made using  $\omega = 1,000$  rpm and  $v = 112$  mm/min displaying a large hook

Details of the hook in Fig. 10 can be examined further using a higher magnification, shown in Fig. 11 (left). It is clear that the hook is fully continued to the very end of the hook, further suggesting that there was little sideward flow to affect the hook. Reducing  $\omega$  value from 1,000 rpm to 500 rpm reduced the pin induced upward flow and thus reduced considerably the  $h$  value from 1.34 mm to 0.28 mm. There must not a sideward flow in that region and  $\gamma$  is close to 0.

The hook features shown in Figs. 10 and 11 can be compared to those in Fig. 8, for welds made using  $\omega = 500$  rpm or 1,000 rpm and  $v = 112$  mm/min. Although the upward flows cannot be clearly compared, it can be concluded that the sideward flow (plastic deformation) was clearly very weak during FSLW of AZ31B. This is consistent with the lack of slip systems in this alloy.

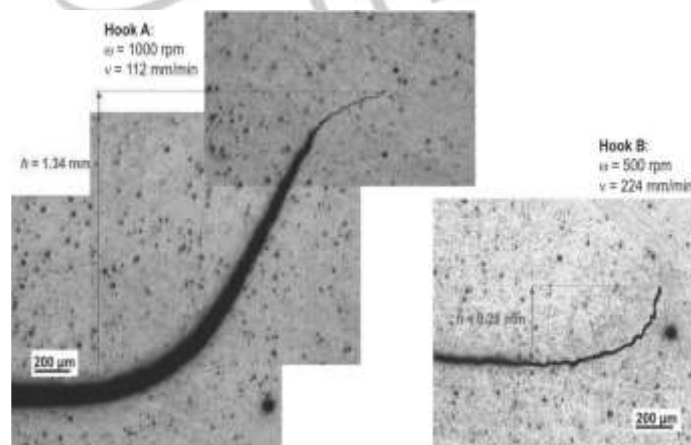


Fig.11. Micrographs of two hooks of AZ31B welds,  $\omega = 1,000$  rpm (left) and  $\omega = 500$  rpm (right),  $v = 112$  mm/min

All Mg lap weld samples fractured in hook locations, as shown in Fig. 12 for two samples with very different hook sizes. Examining these tested samples also suggests little local bending and thus little deformation before the final fracture. This is very different from the high amount of local deformation in Al alloy samples, as already described. Little local deformation and

bending mean that the high stress concentration cannot be relaxed. As suggested in Fig. 8, the effective stress in the hook region should be at least 3 times of the applied stress.

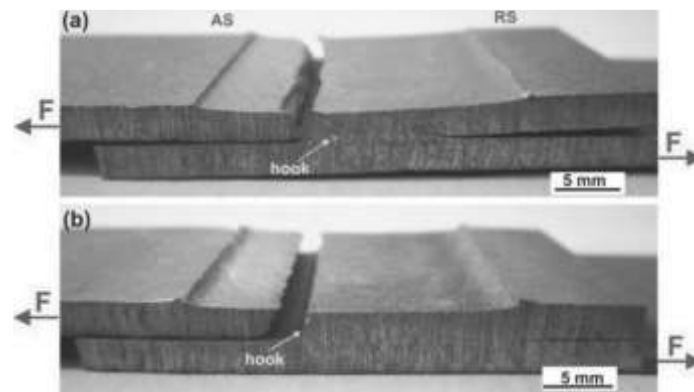


Fig.12. Tensile-shear tested samples of AZ31B welds displaying fracture in hook location (top:  $h = 0.28$  mm, and bottom:  $h = 1.34$  mm)

Microstructures of a tested sample are shown in Fig. 13. The SZ featuring recrystallized grains as the result of the thermomechanical processing during FS is the same as that in the SZ of Al alloy FSL welds, as shown in Fig. 10. The features of deformation in the region adjacent to the fracture surface in AZ31B welds (Fig. 13) are completely different from that in A6060 welds. The grains are not seen elongated suggesting little plastic deformation by slip. Dense twins are observed, suggesting that in the highly stress concentrated region the material deformed by twinning but the total amount of deformation must be quite low before fracturing. These observations are in common with the known deformation behaviors of this alloy, particularly the feature of little necking during tensile testing.

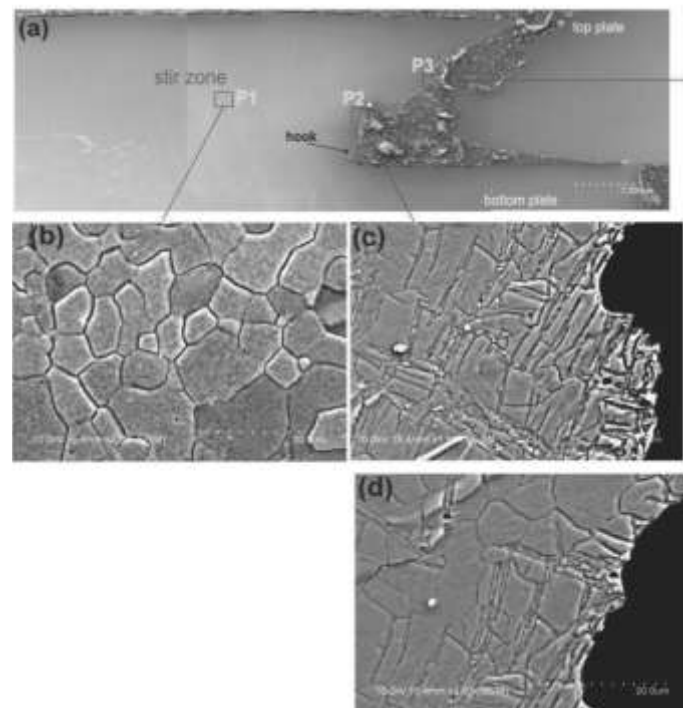


Fig.13. Cross section of an AZ31B tested sample

#### IV. CONCLUSIONS

The size ( $h$ ), orientation ( $\gamma$ ) and continuity of a hook formed during friction stir lap welding (FSLW) of Al-to-Al, using A6060, are FS material flow dependent. While the pin related flow is fundamental for hooking to form,  $\gamma$  and continuity are determined by shoulder related flow. For  $h = 0$ , strength of a weld by tensile-shear testing ( $F_m/w_s$ ) is largely the same as the strength of a bead-on-plate sample. In both cases, FS softening dominates and stress concentration ( $\sigma_c$ ) does not affect  $F_m/w_s$  significantly due to local bending to reduce considerably  $\sigma_c$ . Thinning effect on  $F_m/w_s$  due to hooking can be marked by the effect of softening when  $h$  is not very high. During FSLW of Mg-to-Mg, using AZ31B, shoulder related flow is very weak which results in little reduction in  $h$ , little hook reorientation and little reduction in hook continuity. For Mg-to-Mg welds,  $F_m/w_s$  (lap)  $\ll$   $F_m/w_s$  (butt), due to  $\sigma_c$  effect. The deformation behaviors during FS and tensile-shear testing are consistent with the limited slip systems in Mg.

### REFERENCES

- [1] W.M. Thomas, J.C. Needham, M.G. Murch, P. Templesmith, C.J. Dawes, G B Patent Application No. 9125978.8, 1991.
- [2] S.W. Kallee, D. Lohwasser, Chen Z. (Ed), Friction Stir Welding - from basics to application, Woodhead Publishing, Cambridge, 2010.
- [3] R.S. Mishra, Z.Y. Ma, Friction stir welding and processing, Materials Science and Engineering R 50 (2005) 1-78.
- [4] R. Nandana, T. DebRoy, H.K.D.H. Bhadeshia, Recent advances in friction-stir welding - Process, weldment structure and properties, Progress in Materials Science 53 (2008) 980-1023.
- [5] P.L. Threadgill, A.J. Leonard, H.R. Shercliff, P.J. Withers, Friction stir welding of aluminium alloys, International Materials Review 54 (2009) 49-93.
- [6] L.E. Murr, Structure, synthesis, and chemical reactions of fluorinated cyclopropanes and cyclopropenes, Journal of Materials Engineering and Performance 19 (2010) 1071-1098.
- [7] R. Rai, A. De, H.K.D.H. Bhadeshia, T. DebRoy, Review: friction stir welding tools, Science and Technology of Welding and Joining 16 (2011) 325-342.
- [8] G. Cam, Friction stir welded structural materials: beyond Al-alloys, International Materials Reviews 56 (2011) 1-48.
- [9] Y.N. Zhang, X. Cao, S. Larose, P. Wanjara, Review of tools for friction stir welding and processing, Canadian Metallurgical Quarterly 51 (2012) 250-261.
- [10] L. Cederqvist, A.P. Reynolds, Factors affecting the properties of friction stir welded aluminum lap joints, Welding Journal - Research Supplementary 80 (2001) 281-287.
- [11] M. Ericsson, L. Jin, R. Sandström, Fatigue properties of friction stir overlap welds, International Journal of Fatigue 29 (2007) 57-68.
- [12] D. Fersini, A. Pirondi, Fatigue behaviour of Al2024-T3 friction stir welded lap joints, Engineering Fracture Mechanics 74 (2007) 468-480.
- [13] G. Buffa, G. Campanile, L. Fratini, A. Prisco, Friction stir welding of lap joints: Influence of process parameters on the metallurgical and mechanical properties, Materials Science and Engineering A 519 (2009) 19-26.
- [14] M.K. Yadava, R.S. Mishra, Y.L. Chen, B. Carlson, G.J. Grant, Study of friction stir joining of thin aluminium sheets in lap joint configuration, Science and Technology of Welding and Joining 15 (2010) 70-75.
- [15] L. Dubourg, A. Merati, M. Jahazi, Process optimization and mechanical properties of Friction Stir Lap Welds of 7075-T6 stringers on 2024-T3 skin, Materials and Design 31 (2010) 3324-3330.
- [16] X. Cao, M. Jahazi, Effect of tool rotational speed and probe length on lap joint quality of a friction stir welded magnesium alloy, Materials and Design 32 (2011) 1-11.
- [17] S. Yazdani, Z.W. Chen, G. Littlefair, Effects of friction stir lap welding parameters on weld features on advancing side and fracture strength of A6060-T5 welds, Journal of Materials Science 47 (2012) 1251-1261.